Accepted Manuscript

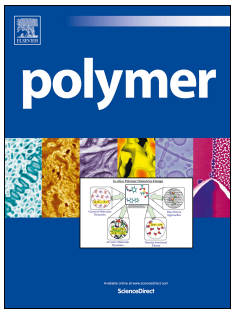

Cross-linked liquid crystalline polybenzoxazines bearing cholesterol-based mesogen side groups

Ying Liu, Jiming Chen, Yongxin Qi, Sheng Gao, Krishnasamy Balaji, Yaoheng Zhang, Qingbin Xue, Zaijun Lu

PII: S0032-3861(18)30391-4

DOI: 10.1016/j.polymer.2018.05.004

Reference: JPOL 20562

To appear in: *Polymer*

Received Date: 13 February 2018

Revised Date: 28 April 2018

Accepted Date: 2 May 2018

Please cite this article as: Liu Y, Chen J, Qi Y, Gao S, Balaji K, Zhang Y, Xue Q, Lu Z, Cross-linked liquid crystalline polybenzoxazines bearing cholesterol-based mesogen side groups, *Polymer* (2018), doi: 10.1016/j.polymer.2018.05.004.

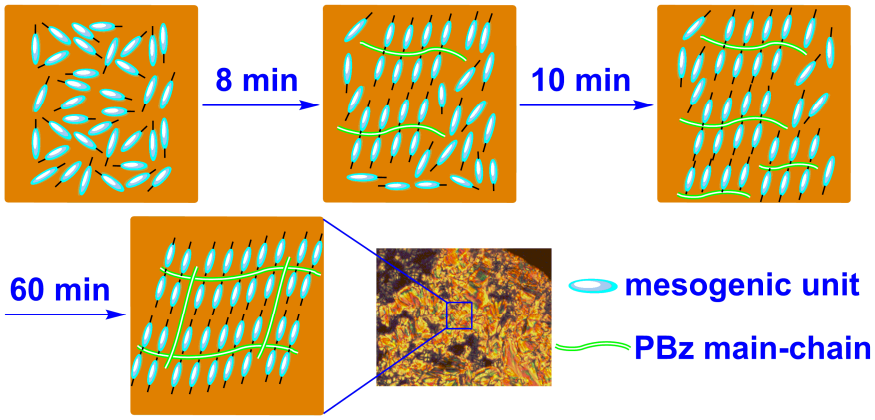

Cross-Linked Liquid Crystalline Polybenzoxazines Bearing Cholesterol-Based Mesogen Side Groups

Ying Liu,[a] Jiming Chen,[b] Yongxin Qi,[b] Sheng Gao,[a] Krishnasamy Balaji,[a] Yaoheng Zhang,[b] Qingbin Xue,[a] and Zaijun Lu*,[a]

[a]Key Laboratory for Special Functional Aggregated Materials of Ministry of Education, School of Chemistry and Chemical Engineering, Shandong University, Jinan, 250100, P. R. China

[b]Institute of Lanzhou Petrochemical Company, PetroChina, Lanzhou, 730060, P. R. China

Abstract

A cross-linked liquid crystalline polybenzoxazine [poly(BA-ac)] was synthesized for the first time from a novel bifunctional benzoxazine monomer (BA-ac) containing cholesterol-based mesogens. The monomer was synthesized using cholesteryl 4-aminobenzoate, bisphenol-A, and paraformaldehyde as raw materials via Mannich reaction. Subsequently, the cross-linked polybenzoxazine bearing cholesterol-based mesogen side groups was obtained through thermally induced ring-opening polymerization of the benzoxazine ring. The study results show that BA-ac is a monotropic smectic C liquid crystal, and poly(BA-ac) contains a smectic C phase structure. The formation of the liquid crystalline structure of poly(BA-ac) is mainly

caused by the strong ability of cholesterol-based mesogen to form liquid crystals and its position on the side group of the cross-linked network. Due to the existence of a liquid crystal structure, poly(BA-ac) has high thermal conductivity. Its coefficient of thermal diffusivity is 31% higher than that of a traditional polybenzoxazine poly(BA-a). Poly(BA-ac) also has high heat-resistance. Its glass transition temperature, 5% and 10% weight loss temperatures are 175 ^{o}C, 306 ^{o}C, and 321 ^{o}C, respectively.

Keywords: polybenzoxazines, liquid crystalline polymers, thermal properties.

Introduction

Heat-resistant polymers are widely used for electronic packaging of electronic components, but most of them have low thermal conductivity, and thus cannot meet the growing demand for heat dissipation of the electronic components. This problem has become one of the bottlenecks restricting the development of integrated circuit and light-emitting diode (LED) lighting. Therefore, there is an urgent need to develop a polymer with high thermal conductivity and high heat-resistance.

At present, the incorporation of liquid crystalline structures into polymers is one of the most effective ways to improve their intrinsic thermal conductivity.[1-6] Liquid crystalline structures can increase the phonon mean free path, and thus highly suppress the phonon scattering and effectively enhance the thermal conductivity. Polybenzoxazine (PBz), which emerged in the past 20 years, is a new type of heat-resistant polymer. It is especially suitable for electronic packaging materials due to its high heat-resistance,

flame retardance, low water absorption, stable dielectric constants, and low cost.[7-10] However, just like ordinary heat-resistant polymers, PBz also has low thermal conductivity. To improve its intrinsic thermal conductivity, some researchers have explored the synthesis of liquid crystalline polybenzoxazine. Several monotropic liquid crystalline benzoxazine monomers (LCBM1 and LCBM2, Fig. 1) were synthesized using phenolic compounds containing cyanobiphenyl mesogens as raw materials via Mannich reaction.[11] Despite the addition of flexible spacers, LCBM1 and LCBM2 did not show any liquid crystalline phases after polymerization. A series of enantiotropic liquid crystalline benzoxazine monomers (7EABn, Fig. 1) were synthesized using a phenolic compound containing aromatic ester and azomethine mesogens as raw material.[12] Although the mesogen aspect ratio of 7EABn was higher than those of LCBM1 and LCBM2, they still did not exhibit a liquid crystalline phase after polymerization. Recently, a series of enantiotropic liquid crystalline benzoxazine monomers (7BEABn, Fig. 1) were synthesized using a liquid crystalline phenolic compound containing aromatic ester, azomethine, and biphenyl mesogens as raw material.[13] The mesogen aspect ratio of 7BEABn was higher than that of 7EABn, resulting in the increment of clearing point and the extension of temperature range of liquid crystalline phase. 7BEAB1 displayed a liquid crystalline phase after curing at 180 ^{o}C for 1 h, but the liquid crystalline phase disappeared after curing to 200 ^{o}C for 1 h.

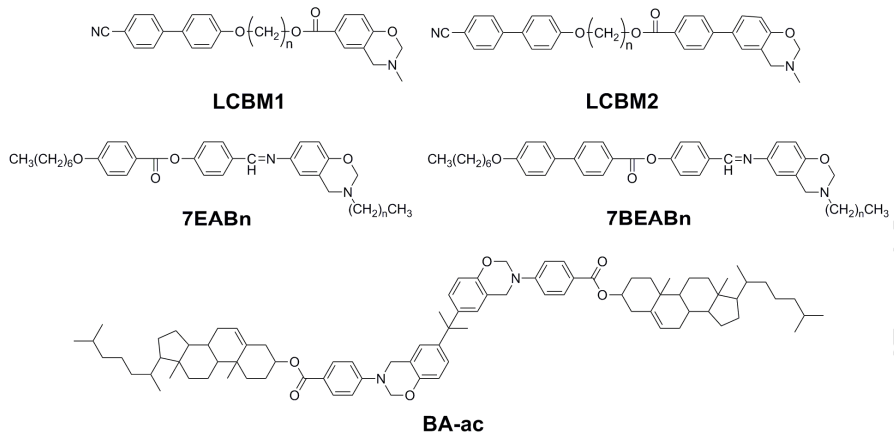

Fig. 1 Chemical structures of LCBMn, 7EABn, 7BEABn, and BA-ac.

In summary, although significant success has been achieved in the synthesis of liquid crystalline benzoxazine monomers, the liquid crystalline phase of the monomers disappears after polymerization, probably because the PBz chain structure is rigid, and prevents the ordered arrangement of the mesogens. Therefore, the synthesis of a liquid crystalline polybenzoxazine has been a challenge. Owing to the fact that cholesterol contains a rigid plate-like structure and a flexible terminal aliphatic chain, its ability to form varieties of liquid crystals is very strong.[14-16] Therefore, herein we choose cholesterol as the mesogenic unit to construct liquid crystalline polybenzoxazine. We hypothesize that the strong short-range interaction between cholesterol mesogens will overcome the rigidity of the PBz chain structure, allowing it to form a liquid crystalline phase. Firstly, a bifunctional liquid crystalline benzoxazine monomer (BA-ac, Fig. 1) based on mesomorphic aromatic amine bearing cholesterol mesogen, bisphenol-A, and paraformaldehyde was synthesized via Mannich reaction. Subsequently, a cross-linked liquid crystalline polybenzoxazine [poly(BA-ac)] containing cholesterol-based mesogen

side groups was obtained through thermally induced ring-opening polymerization of the benzoxazine ring. To the best of our knowledge, this is the first time cross-linked liquid crystalline polybenzoxazine has been synthesized. The development of the liquid crystalline phase during isothermal curing and the thermal properties of the product poly(BA-ac) were also investigated.

Experimental section

Materials

Cholesterol, bisphenol-A, aniline, and paraformaldehyde were supplied by Sinopharm Chemical Reagent Co., Ltd. 4-Nitrobenzoyl chloride was purchased from Shanghai Saen Chemical Technology Co., Ltd. Stannous chloride dihydrate was obtained from Aladdin Industrial Corporation (Shanghai China). All other reagents and solvents were of analytical grade and used as received. 6,6'-(1-Methylethylidene)bis[3-phenyl-3,4-dihydro-2H-1,3-benzoxazine] (BA-a) based on bisphenol-A, aniline, and para-formaldehyde was synthesized according to the literature.[17]

Synthesis of benzoxazine monomer (BA-ac)

The benzoxazine monomer was synthesized in three steps. First, cholesteryl 4-nitrobenzoate (NC) was synthesized by acylation of 4-nitrobenzoyl chloride and cholesterol. Second, the nitro group of NC was reduced to an amino group to obtain cholesteryl 4-aminobenzoate (AC). Finally, the benzoxazine monomer BA-ac was synthesized via Mannich reaction of AC, bisphenol-A, and paraformaldehyde.

Synthesis of cholesteryl 4-nitrobenzoate (NC)

4-Nitrobenzoyl chloride (11.52 g, 62.07 mmol), cholesterol (24.00 g, 62.07 mmol), and pyridine (4.91 g, 62.07 mmol) were refluxed in toluene (180 mL) for 18 h under a nitrogen atmosphere. After solvent removal, the residual was purified by column chromatography (Al_2O_3 gel, 75–150 μm) using eluent CH_2Cl_2:hexane (3:1). White powder (yield: 70%, 23.28 g, 43.42 mmol); mp (liquid crystal) 179 °C (K/Ch). ^{1}H NMR (400 MHz, $CDCl_3$, ppm): δ 8.27 (d, 2H, aromatic protons); 8.19 (d, 2H, aromatic protons), 5.40 (d, 1H, –C=CH–), 4.88 (m, 1H, –COO–CH–), 2.46 (d, 2H, cholesteryl), 2.01-0.83 (m, 38H, aliphatic protons), 0.67 (s, 3H, cholesteryl). FTIR (KBr, cm^{-1}): 1722 (>C=O stretching), 1607 (olefin C=C stretching), 1528 (–NO_2 asymmetric stretching), 1349 (–NO_2 symmetric stretching).

Synthesis of cholesteryl 4-aminobenzoate (AC)

NC (2.00 g, 3.73 mmol) and 8 equivalents of stannous chloride dihydrate (6.74 g, 29.84 mmol) were refluxed in ethanol (100 mL) for 6 h. After cooling to room temperature, the mixture was poured over iced water and the pH value was adjusted to 7–8 using a 5% NaOH aqueous solution. The mixture was extracted with dichloromethane, washed several times with water, and dried over anhydrous $MgSO_4$. After filtration and solvent removal, the crude compound was purified by column chromatography (Al_2O_3 gel, 75–150 μm) using eluent CH_2Cl_2:hexane (3:1). White powder (yield: 63.5%, 1.20 g, 2.37 mmol); mp (liquid crystal) 241 °C (K/Ch).[18] ^{1}H NMR (400 MHz, $CDCl_3$, ppm): δ 7.84 (d, 2H, aromatic protons), 6.62 (d, 2H, aromatic protons), 5.40 (d, 1H, –C=CH–), 4.79 (m,

1H, –COO–CH–), 4.02 (s, 2H, $–NH_2$), 2.43 (d, 2H, cholesteryl), 2.02–0.85 (m, 38H, aliphatic protons), 0.67 (s, 3H, cholesteryl). FTIR (KBr, cm^{-1}): 3489 ($–NH_2$ asymmetric stretching), 3370 ($–NH_2$ symmetric stretching), 1684 (>C=O stretching), 1630 ($–NH_2$ in-plane deformation), 1604 (olefin C=C stretching).

Synthesis of BA-ac

Bisphenol-A (0.68 g, 2.98 mmol), paraformaldehyde (0.39 g, 13.00 mmol), and catalytic amount of triethylamine were added to a solution of AC (3.02 g, 5.97 mmol) in toluene (50 mL). The mixture was stirred for 24 h at reflux temperature. After cooling to room temperature, the precipitate was filtered and white powder was obtained. The crude product was purified by column chromatography (silica gel, 48–75 μm) using eluent CH_2Cl_2 followed by precipitation using excess ethanol. A pure product was obtained after filtration. White powder (yield: 70%, 2.69 g, 2.09 mmol); mp 219 °C. ^{1}H NMR (400 MHz, $CDCl_3$, ppm): δ 7.97 (d, 4H, aromatic protons), 7.08 (d, 4H, aromatic protons), 6.98 (d, 2H, aromatic protons), 6.88 (s, 2H, aromatic protons), 6.75 (d, 2H, aromatic protons), 5.42 (d, 2H, –C=CH–), 5.39 (s, 4H, $O–CH_2–N$), 4.84 (m, 2H, –COO–CH–), 4.66 (s, 4H, $Ar–CH_2–N$), 2.45 (d, 4H, cholesteryl), 1.60 (s, 6H, methyl protons of bisphenol-A), 2.06–0.88 (m, 82H, aliphatic protons), 0.71 (s, 6H, cholesteryl). ^{13}C NMR (100 MHz, $CDCl_3$, ppm): δ 77.69 ($O–CH_2–N$), 50.09 ($Ar–CH_2–N$), 165.70, 152.07, 151.62, 143.52, 139.80, 131.22, 126.63, 124.72, 122.62, 119.73, 116.59, 115.68, 77.21, 74.11, 56.73, 56.19, 42.35, 41.86, 39.54, 38.31, 37.08, 36.67, 36.21, 35.81, 31.95, 31.92, 31.05, 28.24, 27.97, 24.31, 23.86, 22.81, 22.56, 21.08, 19.39, 18.74, 11.88. FTIR

(KBr, cm^{-1}): 1708 (>C=O stretching), 1607 (olefin C=C stretching), 1502 (1,2,4-trisubstituted benzene ring), 1236 (asymmetric stretching of C–O–C in oxazine ring), 959 (out-of-plane C–H stretching of benzene ring attached to oxazine ring). Elemental analysis ($C_{87}H_{118}N_2O_6$): calcd C 81.14, H 9.24, N 2.18; found C 80.43, H 8.71, N 2.02. ESI–MS: calcd for $C_{87}H_{118}N_2O_6$ M^+, *m*/*z* 1287.88; found, *m*/*z* 1287.92 (Fig. S1).

Synthesis of polybenzoxazines

The as-synthesized BA-ac was transferred into a steel mold and thermally cured with a profile as follows: 220 °C for 1 h and 240 °C for 1 h under a pressure of 10 MPa. For comparison, the molten BA-a was cast into a PTFE mold and thermally cured with another profile as follows: 100 °C for 2 h, 140 °C for 2 h, 160 °C for 2 h, and 200 °C for 2 h. The obtained polymers were named as poly(BA-ac) and poly(BA-a), respectively.

Measurements

Fourier transform infrared (FTIR) spectroscopy was performed on a Bruker TENSOR27 spectrometer over a range of 4000 to 400 cm^{-1} at a spectral resolution of 4 cm^{-1}. Samples were prepared using the KBr pellet method.

Proton nuclear magnetic resonance (^{1}H NMR, 400 MHz) and carbon nuclear magnetic resonance (^{13}C NMR, 100 MHz) spectra were recorded on a Bruker AV400 NMR spectrometer in $CDCl_3$ using tetramethylsilane (TMS) as internal standard. Chemical shifts were reported as δ values in ppm.

The electrospray ionization mass spectrometry (ESI-MS) spectra were obtained on an Agilent 6510 Q-TOF mass spectrometer for determining the molecular weight of the

synthesized monomer, and the ionization power used was 135.0 V.

Gel permeation chromatography (GPC) measurements were carried out in tetrahydrofuran (1 mL/min) at 40 ^{o}C using a Waters 515 liquid chromatograph (Milford, MA) equipped with three Styragel columns (HR-3, HR-4, and HR-6) and a refractive-index detector.

Differential scanning calorimetry (DSC) was performed on Netzsch DSC 204 instrument at a heating/cooling rate of 10 °C min^{-1} under a nitrogen atmosphere at a flow rate of 50 mL min^{-1}.

The liquid crystalline textures were observed using a Olympus BX-51 polarizing optical microscope (POM) at a heating/cooling rate of 10 °C min^{-1}, equipped with a Linkam THMSE 600 hot stage and Q-imaging MicroPublisher 5.0 RTV (CCD) camera.

Small/Wide angle X-ray scattering (SAXS/WAXS) was performed on a SAXSess MC2 high flux small-angle X-ray scattering instrument (Anton Paar, Austrian) with Ni-filtered Cu Kα radiation (λ = 0.154 nm), operating at 40 kV and 50 mA. The distance between the sample and detector was 27.8 cm. A standard temperature control unit (Anton-Paar TCS 120) connected to the SAXSess was used to control the temperature at 25 ^{o}C.

Powder X-ray diffraction (XRD) pattern was recorded with a D8 Advance X-ray power diffractometer (Bruker, GM). The work voltage and current were 40 kV and 40 mA, respectively. Cu Ka radiation with a graphite filter was used. The powdered sample was placed on an glass holder and scanned from 8^{o} to 90^{o} at a scan rate of 50^{o} min^{-1}.

The cross-linking density of poly(BA-ac) was estimated by a cross-linking density NMR

analyzer (VTMR20-010V-T, NIUMAG) and was determined from an average of three tests. The powdered sample was placed in a glass tube and measured at 90 °C.

Thermogravimetric analysis (TGA) was performed using a Mettler-Toledo TGA/ADTA851^{e} thermal analyzer. The sample was dried under vacuum at 120 °C for 3 h, and then 6.0−10.0 mg of sample was heated from 30 to 800 °C at a heating rate of 10 °C min^{-1} under a nitrogen atmosphere at a flow rate of 100 mL min^{-1}.

The coefficient of thermal diffusivity of specimens were measured by laser flash diffusivity apparatus (Nano-Flash-Apparatus, LFA 447, Netzsch). The specimen was prepared in a rectangular shape (8 × 8 × 1.2 mm^{3}). All measurements were conducted at room temperature under atmospheric pressure.

Results and Discussion

Synthesis and Characterization of BA-ac

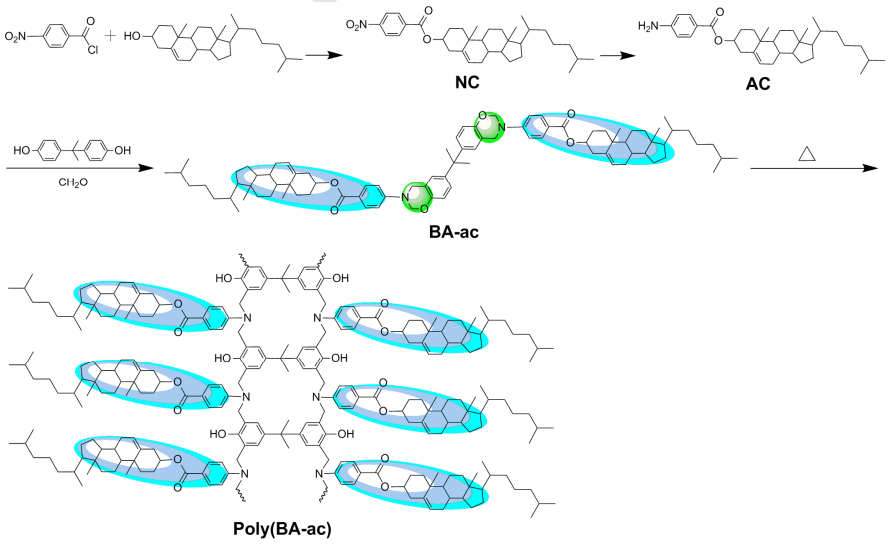

Scheme 1 Synthetic route to BA-ac and its polymer.

Scheme 1 illustrates the synthetic route to BA-ac and its polymer. Firstly, cholesteryl 4-nitrobenzoate (NC) was synthesized by the acylation reaction of 4-nitrobenzoyl chloride and cholesterol, and then the nitro group of NC was reduced to an amino group using stannous chloride as catalyst to obtain cholesteryl 4-aminobenzoate (AC). Subsequently, a bifunctional benzoxazine monomer BA-ac was synthesized via Mannich reaction of AC, bisphenol-A, and paraformaldehyde with a molar ratio of 2: 1: 4 under basic conditions in triethylamine. Finally, a cross-linked polybenzoxazine, poly(BA-ac), was obtained through thermally induced ring-opening polymerization of the benzoxazine ring.

In the absence of triethylamine, the BA-ac reaction system was homogeneous throughout the whole reaction process, but the yield of the product was low. In the presence of triethylamine, the reaction system was homogeneous in the initial stage of the reaction. With the continuation of the reaction, the product was precipitated out from the solution. Precipitation not only favored the purification of the product, but also improved the yield.

Figure 2 (a) shows the ^{1}H NMR spectrum of BA-ac. The resonance signals at 4.66 ppm and 5.39 ppm are assigned to the methylene protons of Ar–CH_2–N– and –O–CH_2–N– in the oxazine ring, respectively, suggesting the formation of oxazine rings. The resonance signals at 5.42 ppm and 4.84 ppm are, respectively, assigned to the olefin proton in cholesterol and the methine proton adjacent to oxygen atom. Moreover, the integrated intensity ratio of those four resonances is 2.00: 1.98: 0.96: 1.04, which is basically

consistent with the theoretical value of 2.00: 2.00: 1.00: 1.00. Additionally, the resonance signal at 1.60 ppm belongs to the methyl proton in bisphenol-A.

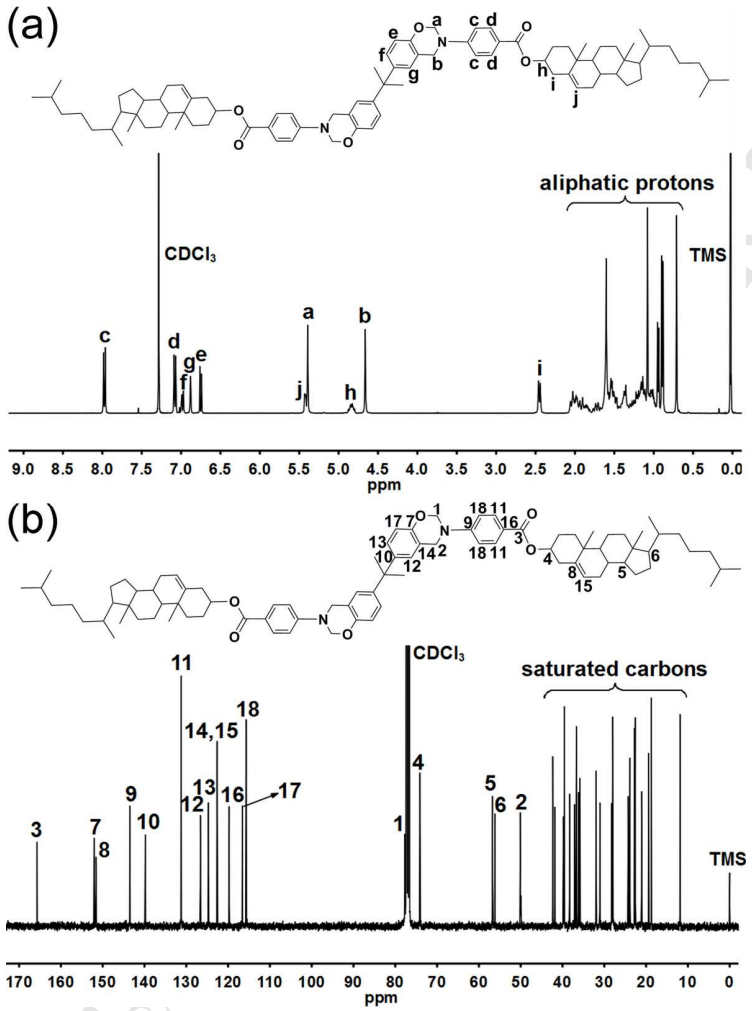

Fig. 2 (a) ^{1}H NMR and (b) ^{13}C NMR spectra of BA-ac.

Figure 2 (b) shows the ^{13}C NMR spectrum of BA-ac. The resonance signals at 50.09 ppm and 77.69 ppm belong to the methylene carbons of Ar–CH_2–N– and –O–CH_2–N– in the oxazine ring, respectively. The resonance signals at 74.11 ppm and 165.70 ppm are, respectively, attributed to the methine carbon adjacent to oxygen atom and the carbonyl carbon.

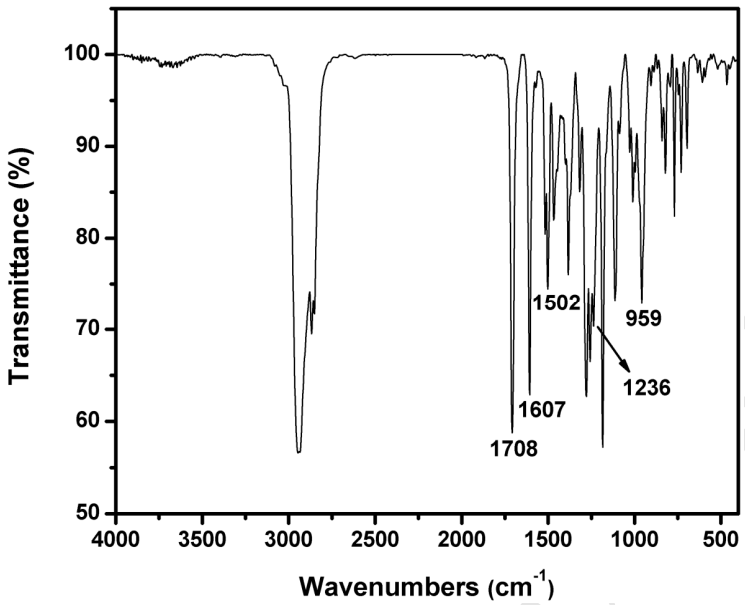

Fig. 3 FTIR spectrum of BA-ac.

Figure 3 shows the FTIR spectrum of BA-ac. The characteristic absorption band of out-of-plane C–H stretching vibration of the benzene ring attached to the oxazine ring appears at 959 cm^{-1}. Furthermore, the absorption bands of the C–O–C asymmetric stretching vibration in the oxazine ring, the 1,2,4-trisubstituted benzene ring vibration, the olefin C=C stretching vibration in cholesterol, and the carbonyl stretching vibration appear at 1236 cm^{-1}, 1502 cm^{-1}, 1607 cm^{-1}, and 1708 cm^{-1}, respectively.

Furthermore, the results of Elemental Analysis and ESI–MS are basically consistent with the calculated values. In sum, BA-ac is successfully synthesized.

Liquid crystalline property of BA-ac

Figure 4 shows the DSC curves of BA-ac upon heating and cooling (Fig. 4 (a)), and the polarized optical micrographs of BA-ac upon cooling (Fig. 4 (b-d)). Upon heating, the endothermic peak at 219 ^{o}C corresponds to the melting point of BA-ac. However, we do

not observe the clearing point of BA-ac. The POM observation shows that an isotropic phase immediately appears after BA-ac melts. Therefore, BA-ac does not show a liquid crystalline phase upon heating. The XRD of BA-ac-240-RT produced by heating BA-ac to 240 °C and then cooling to room temperature (RT) shows that no crystal exists (Fig. S2). Therefore, the exothermic peak at 220 °C upon cooling is the clearing point of the sample, and the exothermic peak at 102 °C is the glass transition temperature of the sample. The temperature range of liquid crystalline phase upon cooling is 102 °C–220 °C. As shown in Fig. 4 (b-d), the area of the bright liquid crystalline region gradually increases with decreasing temperature. Furthermore, the liquid crystalline texture displayed upon cooling is approximately focal-conic texture.

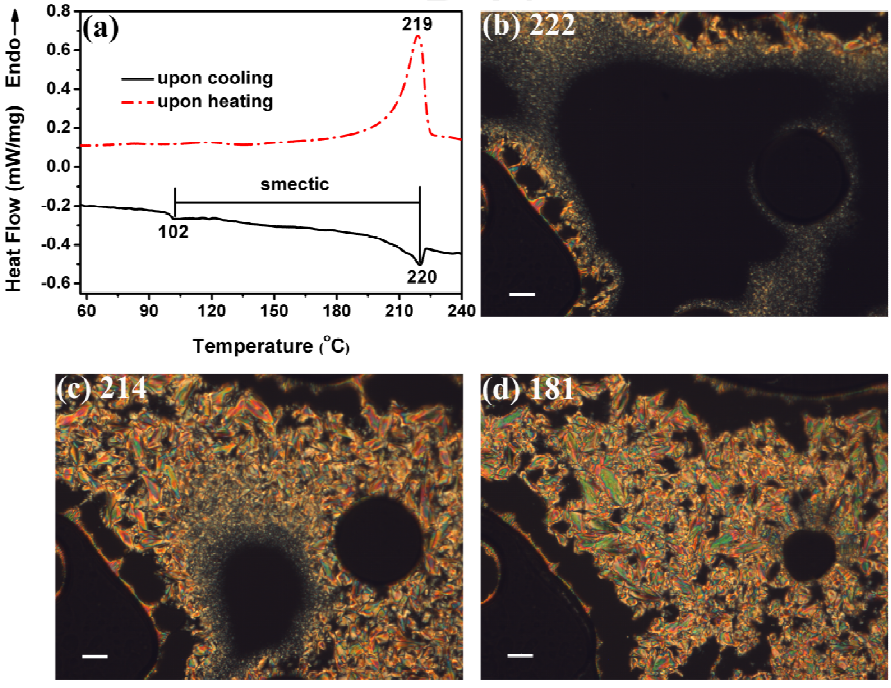

Fig. 4 (a) DSC curves of BA-ac from 57 °C to 240 °C (upon heating) and then cooling to 57 °C (upon cooling). (b-d) Polarized optical micrographs of BA-ac at 222 °C (b), at 214

^{o}C (c), and at 181 ^{o}C (d) upon cooling. Bar, 50 μm.

It should be noted that the the ring-opening polymerization reaction of BA-ac monomer might occur after BA-ac melts. To identify the composition of BA-ac-240-RT, GPC (Fig. S3) and FTIR (Fig. S4) tests were performed. The results show that about 25 wt% of BA-ac monomers undergo ring-opening polymerization and generate BA-ac oligomers. Therefore, the liquid crystalline phase displayed upon cooling should be the result of co-action of the monomers and the oligomers.

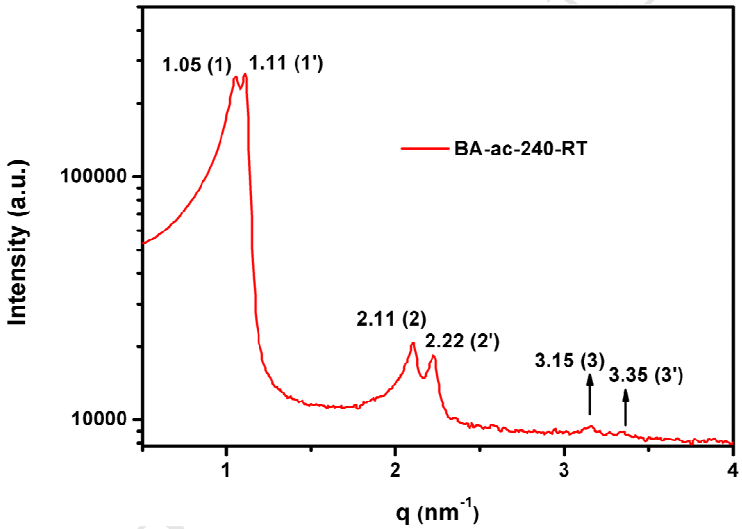

Fig. 5 SAXS profile of BA-ac-240-RT.

To determine the type of liquid crystalline phase upon cooling, small angle X-ray scattering (SAXS) test was carried out. Figure 5 shows the SAXS profile of BA-ac-240-RT. There are two sets of scattering peaks in the figure. Considering that BA-ac-240-RT consists of 75% BA-ac monomers and 25% BA-ac oligomers, the two sets of scattering peaks should be attributed to the monomers and the oligomers, respectively. One set assigned to monomers appears at q_1 = 1.05 nm^{-1}, q_2 = 2.11 nm^{-1},

and q_3 = 3.15 nm^{-1}, and the other set assigned to oligomers appears at q_1' = 1.11 nm^{-1}, q_2' = 2.22 nm^{-1}, and q_3' = 3.35 nm^{-1}. The ratios of the scattering vector q values corresponding to the two sets of scattering peaks are both 1: 2: 3, indicating the formation of two smectic phase structures.[19] According to Bragg's equation: $d = 2\pi / q$ (where d is Bragg spacing, q is scattering vector, and π is ratio of circumference to diameter), the calculated values of the interlayer spacings of the two smectic phases are 5.98 nm (d_1) and 5.66 nm (d_1'), respectively. When BA-ac is in an all-trans conformation and takes a fully extended chain conformation in its liquid crystalline state, the theoretical length for BA-ac is estimated to be 6.23 nm (*L*). Because $d_1/L < 1$, a smectic C (SmC) ordering is proposed to BA-ac monomers.[20] Therefore, BA-ac is a monotropic SmC liquid crystal. The vertical distance between the terminal methyl carbon atoms of the two adjacent cholesterol-based mesogens located at the left and right sides of BA-ac oligomer main-chain, defined as the theoretical width of the oligomer, is approximately 5.80 nm (*S*), assuming a fully extended structure. The layer periodicity d_1' is shorter than *S*. Thus a SmC phase is proposed to BA-ac oligomers.[21]

Liquid crystalline behavior of BA-ac during isothermal curing

Figure 6 shows the POM images of BA-ac after isothermal curing at 220 ^oC for different time intervals. In the initial stage of the curing, the area of the bright crystal region decreases with curing time. When the reaction proceeds for 6 min [Fig. 6 (c)], a large number of approximately bâtonnet-like liquid crystals appear. And more liquid crystals form when the reaction proceeds for 17 min [Fig. 6 (d)]. The liquid crystalline texture is

almost unchanged after 60 min.

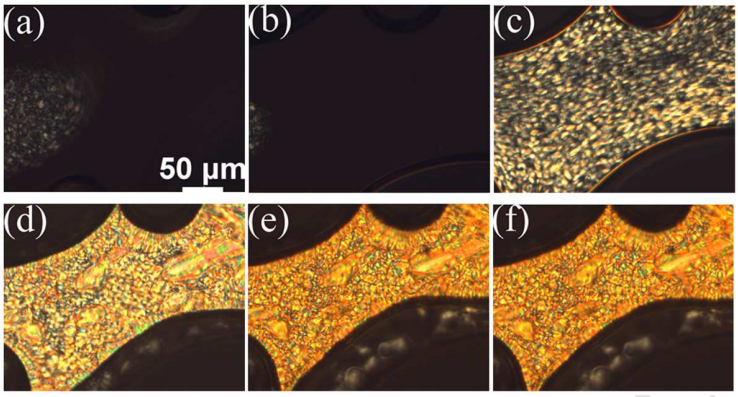

Fig. 6 POM images of BA-ac after isothermal curing at 220 ^{o}C for (a) 1 min, (b) 3 min, (c) 6 min, (d) 17 min, (e) 60 min, and (f) 120 min.

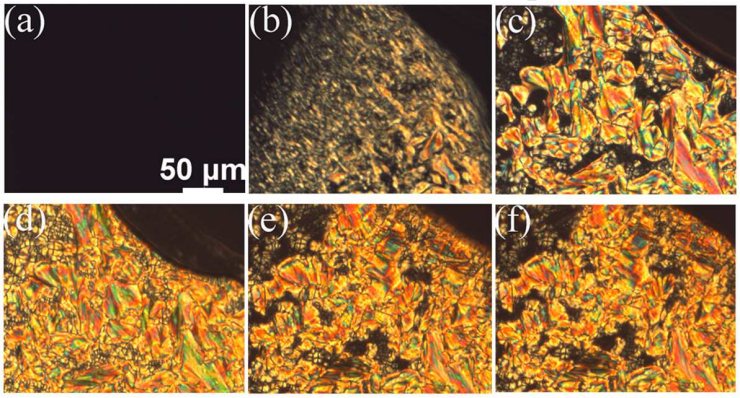

Fig. 7 POM images of BA-ac after isothermal curing at 240 ^{o}C for (a) 1 min, (b) 3 min, (c) 6 min, (d) 17 min, (e) 50 min, and (f) 60 min.

Figure 7 shows the POM images of BA-ac after isothermal curing at 240 ^{o}C for different time intervals. At the beginning of the curing, no bright crystal region is observed because that the system is in an isotropic phase at 240 ^{o}C. When the reaction proceeds for 3 min [Fig. 7 (b)], approximately focal-conic liquid crystals appear. As the reaction progresses, more focal-conic liquid crystals form. The liquid crystalline texture is almost unchanged after 50 min [Fig. 7 (e)]. The formation speed of liquid crystals during

isothermal curing at 240 °C is faster than that of isothermal curing at 220 °C.

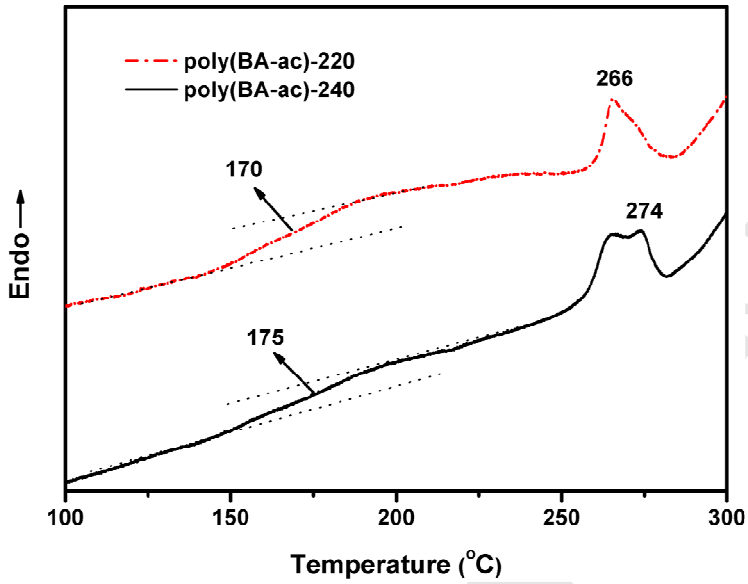

Fig. 8 DSC curves of poly(BA-ac)-220 and poly(BA-ac)-240.

Figure 8 shows the DSC curves of poly(BA-ac)-220 cured at 220 °C for 120 min and poly(BA-ac)-240 cured at 240 °C for 60 min. The glass transition temperature and isotropic temperature of poly(BA-ac)-220 are 170 °C and 266 °C, respectively. Moreover, the isotropic temperature of poly(BA-ac)-220 is verified by the POM observation (Fig. S5). The glass transition temperature of poly(BA-ac)-240 are 175 °C. The endothermic peak at 274 °C is caused by the thermal motion of the liquid crystalline side groups of the poly(BA-ac)-240 cross-linked network. As a result, the liquid crystalline phase of poly(BA-ac)-240 disappears at about 274 °C (Fig. S5).

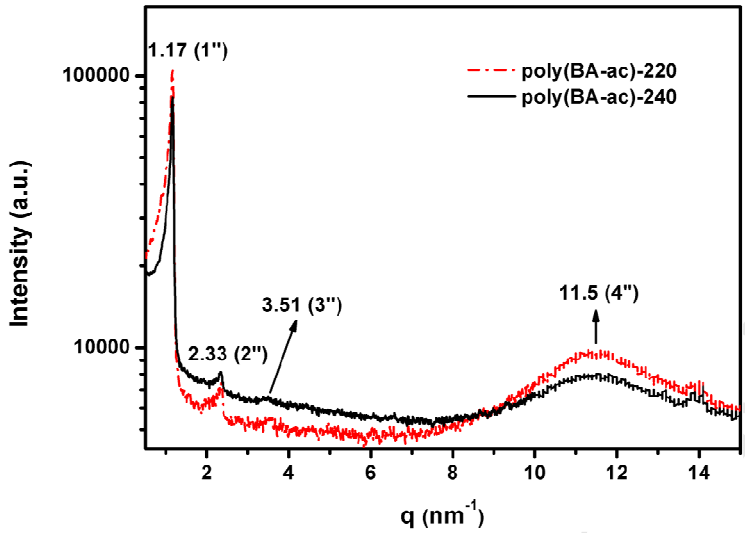

Fig. 9 WAXS profiles of poly(BA-ac)-220 and poly(BA-ac)-240.

To determine the type of the liquid crystalline phase, poly(BA-ac)-220 and poly(BA-ac)-240 were subjected to wide angle X-ray scattering tests (WAXS, Fig. 9). For poly(BA-ac)-220, three sharp scattering peaks appear at $q_1'' = 1.17$ nm^{-1}, $q_2'' = 2.33$ nm^{-1}, and $q_3'' = 3.51$ nm^{-1} in the small angle region. The ratio of the corresponding scattering vector q value is 1: 2: 3, indicating the formation of a smectic phase structure. Furthermore, a diffuse scattering peak related to the lateral packings[22] appears at $q_4'' = 11.5$ nm^{-1} in the wide angle region. According to Bragg's equation, the calculated value of the interlayer spacing of the smectic phase is 5.37 nm (d_1''). The layer periodicity d_1'' is shorter than *S*. Thus a SmC phase is suggested.[21] The position and number of the scattering peaks of poly(BA-ac)-240 are almost the same as poly(BA-ac)-220, so poly(BA-ac)-240 also contains a SmC phase structure.

The solubility tests show that no gelation occurs in poly(BA-ac)-220, and its GPC chromatogram (Fig. S6) shows that poly(BA-ac)-220 is composed of a large amount of

oligomer and a small amount of monomer. However, the solubility tests of the samples cured at 240 ^{o}C show that the gelation occurs when the curing reaction proceeds for 17 min, and the samples are completely cured after 60 min. The GPC tests of the samples cured at 240 ^{o}C (Fig. S7) also confirm this result in more detail. As the curing reaction progresses, the relative content of monomer gradually decreases while the relative content of oligomer gradually increases. The gel appears when the curing reaction proceeds for 17 min.

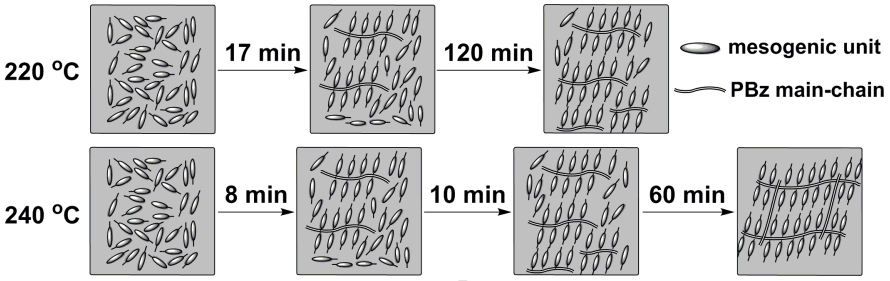

Scheme 2 Development of liquid crystalline phases during isothermal curing.

Scheme 2 shows the evolution of the liquid crystalline phases during isothermal curing. At 220 ^{o}C, the crystal phase of BA-ac monomers disappears, but at 240 ^{o}C, the monomer is initially in an isotropic phase. Over time, the thermally induced ring-opening polymerization generates BA-ac oligomers, which is accompanied by the formation of a liquid crystalline phase of the oligomers. Furthermore, the liquid crystalline phase increases with increasing oligomer content. Finally, a cross-linked network containing liquid crystalline structures forms at 240 ^{o}C *via* the curing reaction.

The poly(BA-ac) can display a liquid crystalline phase after ring-opening polymerization of BA-ac monomers. We believe that there are two main reasons: one is the strong

short-range interaction between the cholesterol-based mesogens, which favors orderly stacking and arrangement of the mesogens. In other words, cholesterol-based mesogen has a strong ability to form a liquid crystalline phase. The other reason is that the cholesterol-based mesogens are located in the side-chain rather than the backbone. Unlike the mesogens connecting to the phenols reported in the literature,[11-13] the cholesterol-based mesogen of poly(BA-ac) connects to the nitrogen atom of a Mannich bridge. This provides greater motional freedom for the cholesterol-based mesogens and favors the formation of liquid crystalline phases. The formation mechanism of the liquid crystalline phase of poly(BA-ac) needs to be further investigated. Other types of mesogens and the effect of different connection sites on the PBz chain are under study in our research group.

Thermal properties of poly(BA-ac)

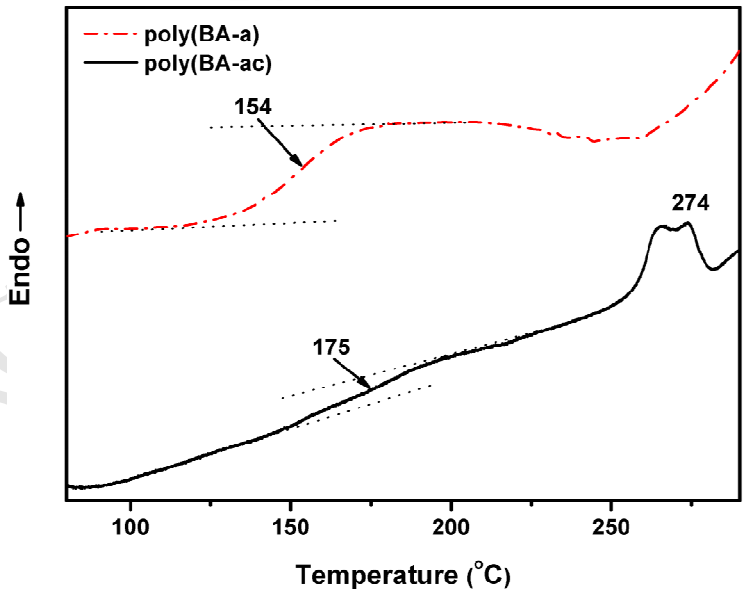

Fig. 10 DSC curves of poly(BA-ac) and poly(BA-a).

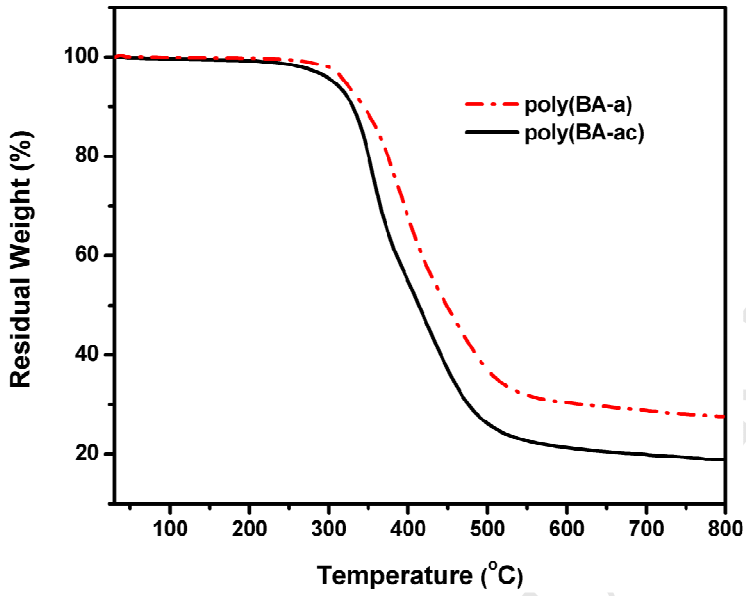

Fig. 11 TGA thermograms of poly(BA-ac) and poly(BA-a).

The conversion of cross-linking reaction of BA-ac after curing at 220 °C for 1 h and at 240 °C for 1 h is estimated by DSC. The results show that all BA-ac monomers are completely cured. Furthermore, the solid-state NMR measurement shows that the cross-linking density of poly(BA-ac) is 3.076×10^{-3} mol mL^{-1}.

Figures 10 and 11 show the DSC curves and TGA thermograms of poly(BA-ac) and poly(BA-a), respectively. The coefficient of thermal diffusivity, glass transition temperature (T_g), 5% weight loss temperature (T_{d5}), and 10% weight loss temperature (T_{d10}) of these two polymers are listed in Table 1. As shown in the Table, the coefficient of thermal diffusivity of poly(BA-ac) is 0.132 mm^2 s^{-1}, which is 31% higher than that of an ordinary polybenzoxazine poly(BA-a). The increment of thermal diffusivity coefficient of poly(BA-ac) is due to the liquid crystalline structure formed by the oriented arrangement of the cholesterol-based mesogens side-chains.[23] The liquid crystalline

structure can effectively enhance the mean free path of phonon vibration, and thus increase the efficiency of phonon's transmission and enhance the intrinsic thermal conductivity of poly(BA-ac).[24] In order to further increase the thermal conductivity of the liquid crystalline polybenzoxazine, a magnetic field can be applied during the monomer curing[3,23] or a conjugated molecular structure can be introduced into the mesogenic unit.[13]

Table 1 Thermal properties of the polymers

Polymer	Coefficient of thermal diffusivity ($mm^2 s^{-1}$)	T_g [a] (^oC)	T_{d5} [b] (^oC)	T_{d10} [c] (^oC)
Poly(BA-ac)	0.132	175	306	321
Poly(BA-a)	0.101	154	330	344

[a] Glass transition temperature. [b] Temperature of 5% weight loss. [c] Temperature of 10% weight loss.

The T_g of poly(BA-ac) is 175 ^oC, which is 21 ^oC higher than that of poly(BA-a), indicating that poly(BA-ac) possesses high heat-resistance. The endothermic peak at 274 ^oC observed from the DSC curve of poly(BA-ac) is attributed to the thermal motion of the liquid crystalline side groups of the poly(BA-ac) cross-linked network, which results in the disappearance of the liquid crystalline phase of poly(BA-ac)-240 (Fig. S8). In addition, the T_{d5} and T_{d10} of poly(BA-ac) are 306 ^oC and 321 ^oC, respectively, which are slightly lower than those of poly(BA-a). To sum up, poly(BA-ac) has a high coefficient

of thermal diffusivity and high heat-resistance.

Conclusions

A cross-linked liquid crystalline polybenzoxazine poly(BA-ac) was successfully prepared for the first time using a bifunctional liquid crystalline benzoxazine monomer BA-ac containing cholesterol-based mesogens. The results show that BA-ac is a monotropic SmC liquid crystal, and poly(BA-ac) contains a SmC phase structure. The evolution of the liquid crystalline phase during isothermal curing involves the disappearance of the crystal phase of BA-ac monomers, and the formation and growth of the liquid crystalline phase of BA-ac oligomers. The liquid crystalline structure gives the polymer high thermal conductivity. The coefficient of thermal diffusivity of poly(BA-ac) is 31% higher than that of poly(BA-a). In addition, the glass transition temperature, and the 5% and 10% weight loss temperatures of poly(BA-ac) are 175 ^{o}C, 306 ^{o}C, and 321 ^{o}C, respectively, indicating that poly(BA-ac) has high heat-resistance. Overall, this work offers a simple and feasible method for the synthesis of cross-linked liquid crystalline polybenzoxazines and provides inspiration on how to obtain liquid crystalline polybenzoxazines.

Acknowledgements

This work is financially supported by Key Research and Development Plan of Shandong Province, China (2017GGX20141) and Shandong Provincial Natural Science Foundation,

China (ZR2018MB022).

Corresponding Author

Correspondence and requests for materials should be addressed to Zaijun Lu, e-mail: z.lu@sdu.edu.cn

Competing financial interests

The authors declare no competing financial interests.

References

[1] J. Shin, M. Kang, T. Tsai, C. Leal, P. V. Braun, D. G. Cahill, *ACS Macro Lett.*, 2016, **5**, 955–960.

[2] M. Wang, J. Wang, H. Yang, B. P. Lin, E. Q. Chen, P. Keller, X. Q. Zhang, Y. Sun, *Chem. Commun.*, 2016, **52**, 4313–4316.

[3] D.-G. Kang, M. Park, D.-Y. Kim, M. Goh, N. Kim, K.-U. Jeong, *ACS Appl. Mater. Interfaces*, 2016, **8**, 30492–30501.

[4] Y. Shoji, R. Ishige, T. Higashihara, J. Morikawa, T. Hashimoto, A. Takahara, J. Watanabe, M. Ueda, *Macromolecules*, 2013, **46**, 747–755.

[5] S. Song, H. Katagi, Y. Takezawa, *Polymer*, 2012, **53**, 4489–4492.

[6] Y. Liu, J. Chen, Y. Zhang, S. Gao, Z. Lu, Q. Xue, *J. Polym. Sci., Part B: Polym. Phys.*, 2017, **55**, 1813–1821.

[7] N. N. Ghosh, B. Kiskan, Y. Yagci, *Prog. Polym. Sci.*, 2007, **32**, 1344–1391.

[8] X. He, J. Wang, Y. Wang, C. Liu, W. Liu, L. Yang, *Eur. Polym. J.*, 2013, **49**, 2759–2768.

[9] Y.-H. Wang, C.-M. Chang, Y.-L. Liu, *Polymer*, 2012, **53**, 106–112.

[10] B. Yao, X. Yan, Y. Ding, Z. Lu, D. Dong, H. Ishida, M. Litt, L. Zhu, *Macromolecules*, 2014, **47**, 1039–1045.

[11] P. Velez-herrera, H. Ishida, *J. Polym. Sci., Part A: Polym. Chem.*, 2009, **47**, 5871–5881.

[12] T. Kawauchi, Y. Murai, K. Hashimoto, M. Ito, K. Sakajiri, T. Takeichi, *Polymer*, 2011, **52**, 2150–2156.

[13] M. Ito, T. Kawauchi, K. Sakajiri, T. Takeichi, *React. Funct. Polym.*, 2013, **73**, 1223–1230.

[14] N. Tamaoki, *Adv. Mater.*, 2001, **13**, 1135–1147.

[15] S.-K. Ahn, L. T. Nguyen le, R. M. Kasi, *J. Polym. Sci., Part A: Polym. Chem.*, 2009, **47**, 2690–2701.

[16] X. Wu, L. Yu, H. Cao, R. Guo, K. Li, Z. Cheng, F. Wang, Z. Yang, H. Yang, *Polymer*, 2011, **52**, 5836–5845.

[17] X. Ning, H. Ishida, *J. Polym. Sci., Part A: Polym. Chem.*, 1994, **32**, 1121–1129.

[18] D. Apreutesei, G. Lisa, H. Akutsu, N. Hurduc, S. Nakatsuji, D. Scutaru, *Appl. Organometal. Chem.*, 2005, **19**, 1022–1037.

[19] F. Zhou, Y. Li, G. Jiang, Z. Zhang, Y. Tu, X. Chen, N. Zhou, X. Zhu, *Polym. Chem.*,

2015, **6**, 6885–6893.

[20] E.-D. Do, K.-N. Kim, Y.-W. Kwon, J.-I. Jin, *Liq. Cryst.*, 2006, **33**, 511–519.

[21] S.-k. Ahn, M. Gopinadhan, P. Deshmukh, R. K. Lakhman, C. O. Osuji, R. M. Kasi, *Soft Matter*, 2012, **8**, 3185–3191.

[22] Y. Jiang, Y. Cong, B. Zhang, *New J. Chem.*, 2016, **40**, 9352–9360.

[23] M. Harada, M. Ochi, M. Tobita, T. Kimura, T. Ishigaki, N. Shimoyama, H. Aoki, *J. Polym. Sci., Part B: Polym. Phys.*, 2003, **41**, 1739–1743.

[24] Y. Kim, H. Yeo, N.-H. You, S. G. Jang, S. Ahn, K.-U. Jeong, S. H. Lee, M. Goh, *Polym. Chem.*, 2017, **8**, 2806–2814.

1. A mesomorphic benzoxazine monomer based on mesomorphic aromatic amine is synthesized.

2. A cross-linked liquid crystalline polybenzoxazine is obtained for the first time.

3. The liquid crystalline structure endows the polybenzoxazine high thermal conductivity.